

Geometric semimetals and their simulation in synthetic matter

Yu-Ping Lin^{1,*} and Giandomenico Palumbo^{2,†}

¹*Department of Physics, University of California, Berkeley, California 94720, USA*

²*School of Theoretical Physics, Dublin Institute for Advanced Studies,
10 Burlington Road, Dublin 4 D04 C932, Ireland*

(Dated: May 9, 2024)

Topological semimetals, such as the Weyl and Dirac semimetals, represent one of the most active research fields in modern condensed matter physics. The peculiar physical properties of these systems mainly originate from their underlying symmetries, emergent relativistic dispersion, and band topology. In this Letter, we present a different class of gapless systems in three dimensions, dubbed *geometric semimetals*. These semimetals are protected by the generalized chiral and rotation symmetries, but are topologically trivial. Nevertheless, we show that their band geometry is nontrivial, as evidenced by the nonzero quantum metric trace with possible quantization. The possible realization in synthetic-matter experiments is also discussed.

Introduction. The search for novel topological semimetals has been a mainstream of modern condensed matter physics. Starting with the Weyl and Dirac semimetals in three dimensions (3D) [1–3], which host linear band crossing points (LBCPs) of nondegenerate and doubly degenerate bands, respectively, the exploration has embraced various generalizations of BCs. One important family features the multifold LBCPs with multiple Fermi velocities [4–21], which are the higher-spin versions of Weyl and Dirac semimetals. Other families include the BCPs with higher-order dispersions, such as the quadratic BCPs (QBCPs) [22–24], and the higher-dimensional BCs in the forms of lines [1, 20, 25–31] or surfaces [20, 28, 30, 32, 33]. Importantly, the BCs in topological semimetals are associated with suitable topological invariants, which depend mainly on the underlying symmetries and spatial dimensions. These topological invariants can be derived from the Abelian and non-Abelian Berry connections as gauge-invariant quantities. In 3D (5D), the Weyl and chiral multifold semimetals are the momentum-space Dirac (Yang) monopoles with first (second) Chern numbers [19, 20, 34, 35]. Similarly, 2D and 4D Dirac-like points can act as vortices [20] and tensor monopoles [36, 37], respectively. Other examples include the Euler numbers of LBCPs [29, 38–42] and \mathbb{Z}_2 numbers of nodal loops [27, 31, 43, 44] under combined inversion and time-reversal (PT) symmetry, as well as the delicate topology of QBCPs [24]. While many topological semimetals have been discovered in quantum materials, recent experiments have demonstrated successful simulations in synthetic matter, including superconducting quantum circuits [45, 46], diamond nitrogen-vacancy centers [47, 48], and ultracold atoms [49].

Despite the ubiquitous importance of band topology to the BCs, there exist topologically trivial semimetals which do not carry any topological invariant. Particular examples include the 3D Kane-fermion model [50–53] and 2D α - T_3 model [54–56] under rotation symmetry, where the LBCPs are attached with middle flat bands. On the other hand, a LBCP of PT -symmetric nonde-

generate bands with $T^2 = 1$ generally hosts a trivial band topology, since the Berry connection vanishes in the “real” band eigenstates (for doubly or quadruply degenerate bands, the LBCPs could be Euler semimetals instead). A natural question then occurs: *Can topologically trivial semimetals receive protection from any symmetry and support nontrivial physical quantities with possible quantization?*

The goal of our *Letter* is to provide an affirmative answer to this question. We introduce a general semimetallic model in 3D, where a topologically trivial BCP occurs between multiple dispersive and degenerate middle flat bands (Fig. 1). Importantly, the semimetals in our model are protected by the generalized chiral and rotation symmetries. Despite trivial band topology, we show that these semimetals host nontrivial structures related to band geometry. The characterization of band geometry lies in the quantum metric [19, 20, 57–60], which contributes to various observable quantities and physical phenomena [45, 47, 48, 60–101]. Note that nontrivial band geometry occurs more ubiquitously than nontrivial band topology: while the latter is strictly related to quantized topological invariants, the former is broadly manifest under nonzero quantum metric. We focus on the quantum metric trace and derive its nontrivial struc-

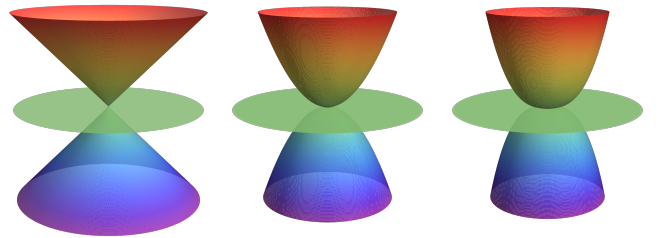


FIG. 1. Geometric semimetals. (Left to right) The band structures in the two-spin-sector $N = 2$ models with spins $(s_1, s_2) = (0, 1)$, $(0, 2)$, and $(1, 2)$. The dispersive bands are nondegenerate, while the flat-band degeneracies are 2, 4, and 6, respectively.

tures with possible quantization [19, 20]. Given nontrivial band geometry under trivial band topology, we dub our systems *geometric semimetals* to distinguish them from the topological ones. We further show that the variants of our model constitute a broader family, which includes the 3D Kane-fermion model [50–53] and 2D α - T_3 model [54–56] under rotation symmetry. Finally, we discuss the possible experimental realization in synthetic matter.

General model. We begin by introducing the general model for a class of geometric semimetals in 3D. Our model is a minimal model about a reference point in momentum space. It can be directly simulated in synthetic-matter experiments [45–49], or serve as a low-energy $k \cdot p$ theory of suitable lattice models for quantum materials. Without loss of generality, we set the reference point at the momentum-space origin. The central spirit is to couple different spin sectors under the SU(2) spin-orbit-coupled rotation symmetry. Correspondingly, the relevant ingredients are the total-angular-momentum states

$$|v_{jm_j\mathbf{k}}^{sl}\rangle = \sum_{m_s=-s}^s \sum_{m_l=-l}^l \sqrt{4\pi} \langle slm_s m_l | jm_j \rangle Y_{lm_l}(\hat{\mathbf{k}}) |sm_s\rangle \quad (1)$$

from the additions of spin states $|sm_s\rangle$ and orbital spherical harmonics $Y_{lm_l}(\hat{\mathbf{k}})$ with Clebsch-Gordan coefficients $\langle slm_s m_l | jm_j \rangle$. The respective angular momenta and axial components are s, l, j and $m_{s,l,j}$, which are set as integers in our analysis. Meanwhile, $\hat{\mathbf{k}}$ is the directional unit vector of momentum $\mathbf{k} = (k_1, k_2, k_3) = k\hat{\mathbf{k}}$ with magnitude k . For the spin sector α with spin s_α , the $j_\alpha = 0$ state with $l_\alpha = s_\alpha$

$$|v_{\alpha\mathbf{k}}^1\rangle = |v_{00\mathbf{k}}^{s_\alpha s_\alpha}\rangle \quad (2)$$

is the only rotation symmetric state in the spin-orbit-coupled Hilbert space. This motivates us to consider the $j = 0$ projectors between different spin sectors $\alpha \neq \beta$

$$T_{\alpha\beta\mathbf{k}} = k^{s_\alpha} |v_{\alpha\mathbf{k}}^1\rangle \langle v_{\beta\mathbf{k}}^1 | k^{s_\beta}, \quad (3)$$

which are the rotation symmetric couplings of our interest. We thus define the model with N spin sectors by the Hamiltonian

$$\mathcal{H}_{\mathbf{k}} = \begin{pmatrix} 0 & T_{12\mathbf{k}} & \dots & T_{1N\mathbf{k}} \\ T_{21\mathbf{k}} & 0 & \ddots & \vdots \\ \vdots & \ddots & \ddots & T_{(N-1)N\mathbf{k}} \\ T_{N1\mathbf{k}} & \dots & T_{N(N-1)\mathbf{k}} & 0 \end{pmatrix} \quad (4)$$

with $T_{\alpha\beta\mathbf{k}} = T_{\beta\alpha\mathbf{k}}^\dagger$. Note that the diagonal blocks are zero, implying the sole manifestation of the off-diagonal couplings.

Having constructed the general model, we proceed to calculate the dispersion energies $\epsilon_{\mathbf{k}}$ and study the band

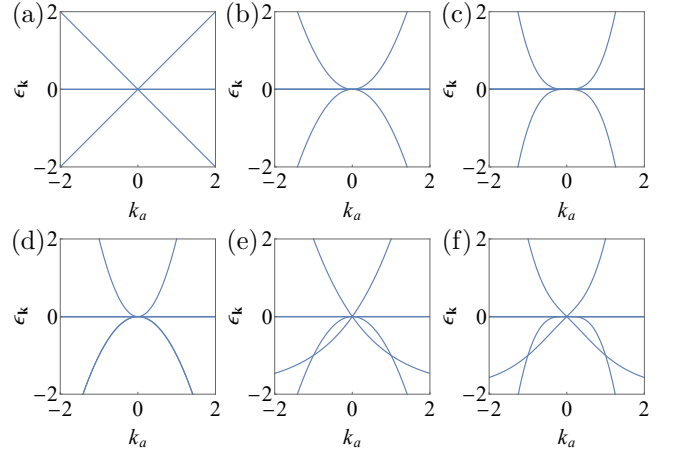


FIG. 2. The band structures in the (a)-(c) $N = 2$ models with $(s_1, s_2) = (0, 1), (0, 2), (1, 2)$ and (d)-(f) $N = 3$ models with $(s_1, s_2, s_3) = (1, 1, 1), (0, 1, 1), (0, 1, 2)$. All of the dispersive bands are non-degenerate, except for the doubly degenerate negative bands in (d). The flat-band degeneracies are 2, 4, 6, 6, 4, 6 in (a)–(f), respectively. Due to rotation symmetry, the momentum component k_a can be chosen along any direction.

structure (Fig. 2). To secure the BCP at $\epsilon_0 = 0$, we assume that the spin-0 sector appears at most once. Summing the Hilbert-space dimensions $2s_\alpha + 1$ of all spin sectors, the model contains $\sum_{\alpha=1}^N (2s_\alpha + 1)$ bands. The first observation is the bundle of middle flat bands with zero dispersion $\epsilon_{\mathbf{k}}^0 = 0$. These flat bands are composed of the states

$$|u_{\alpha\mathbf{k}}^n\rangle = \dots \oplus |0\rangle \oplus |v_{\alpha\mathbf{k}}^n\rangle \oplus |0\rangle \oplus \dots \quad (5)$$

with $n = 0$, where the states $|v_{\alpha\mathbf{k}}^0\rangle$ are orthogonal to the $j_\alpha = 0$ state $\langle v_{\alpha\mathbf{k}}^1 | v_{\alpha\mathbf{k}}^0 \rangle = 0$ in the spin sector α . The zero dispersion follows from the projector condition $T_{\alpha\beta\mathbf{k}} |v_{\beta\mathbf{k}}^0\rangle = 0$. Since the subspace $\{|v_{\alpha\mathbf{k}}^0\rangle\}$ is $2s_\alpha$ -dimensional in each spin sector, the total degeneracy of these flat bands is $\sum_{\alpha=1}^N 2s_\alpha$.

There remain N dispersive bands for us to investigate. These bands are composed of the $j_\alpha = 0$ states

$$|u_{\mathbf{k}}\rangle = \sum_{\alpha=1}^N u_{\alpha\mathbf{k}} |u_{\alpha\mathbf{k}}^1\rangle, \quad (6)$$

where the amplitudes $u_{\alpha\mathbf{k}}$ are generally k -dependent. Projected to the $j_\alpha = 0$ basis $\{|u_{\alpha\mathbf{k}}^1\rangle\}_{\alpha=1,2,\dots,N}$, the dispersive Hamiltonian reads

$$\tilde{\mathcal{H}}_{\mathbf{k}} = \begin{pmatrix} 0 & k^{s_1+s_2} & \dots & k^{s_1+s_N} \\ k^{s_2+s_1} & 0 & \ddots & \vdots \\ \vdots & \ddots & \ddots & k^{s_{N-1}+s_N} \\ k^{s_N+s_1} & \dots & k^{s_N+s_{N-1}} & 0 \end{pmatrix}. \quad (7)$$

The diagonalization of this Hamiltonian is complicated in general. Nevertheless, if all effective couplings have the

same power $s_\alpha + s_\beta = p$, we can find simple solutions with k -independent band eigenstates. This condition applies to all $N = 2$ models, as well as the $N > 2$ models with the same spin $s_{\alpha=1,2,\dots,N} = p/2$. The corresponding band eigenstates are

$$\begin{aligned} &1 \text{ positive band: } \epsilon_{\mathbf{k}}^+ = (N-1)k^p, \\ &(N-1) \text{ negative band: } \epsilon_{\mathbf{k}}^- = -k^p. \end{aligned} \quad (8)$$

The positive band is always non-degenerate, where the eigenstate has a constant amplitude $u_{\alpha\mathbf{k}} = 1/\sqrt{N}$. Meanwhile, the negative band is non-degenerate in the $N = 2$ model with $u_{(\alpha=1,2)\mathbf{k}} = (-1)^{\alpha-1}/\sqrt{2}$.

Symmetry protection. It is important to understand whether the semimetals are protected by any symmetry. To confirm such a protection, we examine whether a mass term

$$\mathcal{H}_m = m \begin{pmatrix} h_{11} & h_{12} & \dots & h_{1N} \\ h_{21} & h_{22} & \ddots & \vdots \\ \vdots & \ddots & \ddots & h_{(N-1)N} \\ h_{N1} & \dots & h_{N(N-1)} & h_{NN} \end{pmatrix} \quad (9)$$

with nonzero mass $m \neq 0$ and constant representations $h_{\alpha\beta} = h_{\beta\alpha}^\dagger$ is symmetry-allowed to open a mass gap. Our first target is the chiral symmetry, which plays a crucial role in many semimetals. Interestingly, our general model respects a generalized version of chiral symmetry $\sum_{q=0}^{N-1} U_{S,N}^q \mathcal{H}_{\mathbf{k}} (U_{S,N}^\dagger)^q = 0$ [102, 103], where $U_{S,N} = \bigoplus_{\alpha=1}^N \exp[i2\pi(\alpha-1)/N]$ is the generalized chiral unitary operator. In particular, the $N = 2$ models respect the standard chiral symmetry $U_S \mathcal{H}_{\mathbf{k}} U_S^\dagger = -\mathcal{H}_{\mathbf{k}}$ with $U_S = U_{S,2}$ [34]. The generalized chiral symmetry imposes a strong constraint on the mass term. While nonzero diagonal representations are forbidden $h_{\alpha\alpha} = 0$, the off-diagonal ones $h_{\alpha\beta}$ with $\alpha \neq \beta$ are generally allowed. The protection of the semimetals requires additional symmetry to fully reject the remaining terms.

Among various other symmetries, the discrete and continuous rotation symmetries are relevant to some topological semimetals [104–106]. It turns out that the $SU(2)$ spin-orbit-coupled rotation symmetry completes the demanded protection in our model. Under the rotation symmetry, the constant representations are only allowed in the identity forms $h_{\alpha\beta} = 1$ with $s_\alpha = s_\beta$. If all of the spin sectors carry different spins, $s_\alpha \neq s_\beta$ for $\alpha \neq \beta$, the rotation symmetry forbids all nonzero off-diagonal constant representations $h_{\alpha\beta} = 0$. Therefore, the semimetals are protected by the generalized chiral and rotation symmetries. On the other hand, the mass term is allowed if there are different spin sectors $\alpha \neq \beta$ with the same spin $s_\alpha = s_\beta$. In this case, the semimetals lose the protection even if both symmetries are present. Note that BCPs with continuous rotation symmetries can be realized in the synthetic-matter experiments [45–49]. In the quantum materials with lattice structures, the global symmetries are discrete and the continuous rotation symmetries

can be low-energy approximations around some BCPs. These low-energy approximate symmetries, known as the quasisymmetries, have recently been shown to play an important role in gapless topological materials [107, 108].

One may wonder whether the semimetals receive protection in the tenfold-way classification [34]. Our model respects the time-reversal symmetry $T\mathcal{H}_{\mathbf{k}}T^{-1} = \mathcal{H}_{-\mathbf{k}}$ with the symmetry operator $T = U_T\mathcal{K}$. Here \mathcal{K} is the complex conjugate operator, and the unitary operator $U_T = \bigoplus_{\alpha=1}^N \sum_{m_{s_\alpha}=-s_\alpha}^{s_\alpha} (-1)^{s_\alpha+m_{s_\alpha}} |s_\alpha(-m_{s_\alpha})\rangle \langle s_\alpha m_{s_\alpha}|$ meets the relations of complex conjugate $Y_{lm_l}(\hat{\mathbf{k}}) = (-1)^{m_l} Y_{l(-m_l)}^*(\hat{\mathbf{k}})$ and opposite momentum $Y_{lm_l}(\hat{\mathbf{k}}) = (-1)^l Y_{lm_l}(-\hat{\mathbf{k}})$ for orbital spherical harmonics. Note that the time-reversal operator satisfies $T^2 = 1$. For the $N > 2$ models, the absence of chiral symmetry indicates the AI class. Despite the \mathbb{Z} classification, the mass term with $h_{\alpha\beta m_{s_\alpha} m_{s_\beta}} = (-1)^{s_\alpha+m_{s_\alpha}+s_\beta+m_{s_\beta}} h_{\alpha\beta(-m_{s_\alpha})(-m_{s_\beta})}^*$ is allowed to gap the semimetal. On the other hand, the $N = 2$ models obey the particle-hole symmetry $C\mathcal{H}_{\mathbf{k}}C^{-1} = -\mathcal{H}_{-\mathbf{k}}$ with $C = U_C\mathcal{K}$ and $U_C = \bigoplus_{\alpha=1}^2 \sum_{m_{s_\alpha}=-s_\alpha}^{s_\alpha} (-1)^{(\alpha-1)+s_\alpha+m_{s_\alpha}} |s_\alpha(-m_{s_\alpha})\rangle \langle s_\alpha m_{s_\alpha}|$. The condition $C^2 = 1$ assigns the models to the BDI class without nontrivial classification. Based on these results, we find no protection of the semimetals in the tenfold-way classification.

Our model also satisfies the reality condition (which is real in the real basis) of PT symmetry $(PT)\mathcal{H}_{\mathbf{k}}(PT)^{-1} = \mathcal{H}_{\mathbf{k}}$, which enforces the vanishing of Berry fluxes. Here the symmetry operator $PT = U_{PT}\mathcal{K}$ with $U_{PT} = \bigoplus_{\alpha=1}^N \sum_{m_{s_\alpha}=-s_\alpha}^{s_\alpha} (-1)^{m_{s_\alpha}} |s_\alpha(-m_{s_\alpha})\rangle \langle s_\alpha m_{s_\alpha}|$ meets the complex conjugate relation of orbital spherical harmonics. Under the PT symmetry, the reality condition $h_{\alpha\beta m_{s_\alpha} m_{s_\beta}} = (-1)^{m_{s_\alpha}+m_{s_\beta}} h_{\alpha\beta(-m_{s_\alpha})(-m_{s_\beta})}^*$ does not entirely rule out the mass term. Therefore, the semimetals do not receive protection from the PT symmetry.

Nontrivial band geometry. We have demonstrated the symmetry protection of the semimetals in our model. A natural question is whether nontrivial band properties related to this protection exist. For the topological semimetals, the robustness is usually linked to certain topological invariants. For example, a chiral semimetal can exhibit Abelian Berry flux $\mathbf{B}_{\mathbf{k}} = \nabla_{\mathbf{k}} \times \mathbf{A}_{\mathbf{k}}$ with Berry gauge field (or connection) $\mathbf{A}_{\mathbf{k}} = \langle u_{\mathbf{k}} | i\nabla_{\mathbf{k}} | u_{\mathbf{k}} \rangle$, leading to a finite Chern number $C = (1/2\pi) \oint d\mathbf{S}_{\mathbf{k}} \cdot \mathbf{B}_{\mathbf{k}}$ under the surface integral around the BCP [1]. However, the bands in our model, such as the nondegenerate positive band, exhibit zero Berry flux and trivial band topology under the PT symmetry. This feature can be observed from the spherical harmonics in the band eigenstates, which are the monopole harmonics with zero Berry monopole [109, 110].

Despite trivial band topology, our model exhibits nontrivial structures in the band geometry. This nontriviality is characterized by the nonzero quantum metric of

the band eigenstates [19, 20, 111]

$$g_{ab\mathbf{k}} = \frac{1}{2} \langle u_{\mathbf{k}} | \{r_{a\mathbf{k}}, r_{b\mathbf{k}}\} | u_{\mathbf{k}} \rangle. \quad (10)$$

Here a, b are the spatial indices, and the position $\mathbf{r}_{\mathbf{k}} = i\nabla_{\mathbf{k}} - \mathbf{A}_{\mathbf{k}}$ is a momentum-space covariant derivative under the Berry gauge field. An important task is to further understand the nontrivial band geometry. Notably, the quantum metric trace

$$\text{Tr}g_{\mathbf{k}} = \langle u_{\mathbf{k}} | |\mathbf{r}_{\mathbf{k}}|^2 | u_{\mathbf{k}} \rangle \quad (11)$$

represents the momentum-space dual kinetic energy under a position-momentum duality [19, 20]. With the rotation symmetry, the dual energy is dualized to the free-electron kinetic energy on a spherical shell. This implies the sole contribution from the dynamical angular momentum $\Lambda_{\mathbf{k}} = \mathbf{r}_{\mathbf{k}} \times \mathbf{k}$

$$\text{Tr}g_{\mathbf{k}} = \frac{|\Lambda_{\mathbf{k}}|^2}{k^2}. \quad (12)$$

The absence of Berry monopole implies the equivalence between dynamical and orbital angular momenta $\Lambda_{\mathbf{k}} = \mathbf{L}_{\mathbf{k}}$ [19, 20, 112–114]. Correspondingly, the dual energy exhibits the quantization $|\Lambda_{\mathbf{k}}|^2 = l_{\alpha}(l_{\alpha} + 1) = s_{\alpha}(s_{\alpha} + 1)$ in the spin sector α . Summing over all spin sectors, the quantum metric trace represents the total dual energy

$$\text{Tr}g_{\mathbf{k}} = \frac{1}{k^2} \sum_{\alpha=1}^N |u_{\alpha\mathbf{k}}|^2 s_{\alpha}(s_{\alpha} + 1). \quad (13)$$

Note that this result is positively definite, indicating the general presence of nontrivial band geometry in our model. Given nontrivial band geometry under trivial band topology, we name these semimetals as *geometric semimetals*.

In general, nontrivial band geometry is not necessarily related to quantized invariants. However, it is worth searching for possible quantization under certain conditions, such as the rotation symmetry. Motivated by the topological invariants, such as the Chern number, we consider the surface integral of quantum metric trace around the BCP [19]

$$G = \frac{1}{2\pi} \oint d\mathbf{S}_{\mathbf{k}} \cdot \hat{\mathbf{k}} \text{Tr} g_{\mathbf{k}}. \quad (14)$$

This integral generally varies with the choice of surface, since the amplitudes $u_{\alpha\mathbf{k}}$ depend on k . Nevertheless, the results become quantized constants in the $N = 2$ models

$$G = \sum_{\alpha=1}^2 s_{\alpha}(s_{\alpha} + 1). \quad (15)$$

The quantization with respect to angular momentum reflects the protection by rotation symmetry (and the standard chiral symmetry). Therefore, this quantity may

serve as a *geometric invariant* [19] for the geometric semimetals. As the simplest examples, we obtain the quantized geometric invariants $G = 2, 6,$ and 8 for $(s_1, s_2) = (0, 1), (0, 2),$ and $(1, 2),$ respectively.

Note that nontrivial band geometry is also present in the degenerate flat bands, which involves the non-Abelian quantum metric [60, 83]. Since the flat-band eigenstates $|u_{\alpha\mathbf{k}}^0\rangle$ are not rotation symmetric, the result is generally anisotropic.

In synthetic-matter experiments, the quantum metric can be extracted directly from the transition rates $\Gamma_a \sim V^2 g_{aa\mathbf{k}}$ under sudden quench or periodic drive at strength V along direction a [46–49, 80]. With this accessibility, the nontriviality and possible quantization can be examined for the quantum metric trace $\text{Tr}g_{\mathbf{k}}$ and geometric invariant G , which are physical observables by themselves. On the other hand, the quantum metric trace $\text{Tr}g_{\mathbf{k}}$ is related to the spread of Wannier functions [61], whose gauge-invariant lower bound is supported by the integral of geometric invariant $\Omega_I \sim \int_{\mathbf{k}} \text{Tr}g_{\mathbf{k}} \geq \int_0^{\Lambda_k} dk (2\pi G)$, with a momentum cutoff Λ_k around the nodal point [19]. The corresponding physical observables, including linear injection conductivity [88, 90] and superfluid stiffness [65], are relevant to the quantum-material experiments. Through a direct calculation (see Supplemental Material [115]), we confirm that the linear injection conductivity indeed receives nontrivial contribution from band geometry in geometric semimetals. Meanwhile, the superfluid stiffness acquires a geometric contribution $\text{Tr}D_{\text{geom}}^S \gtrsim 2 \int_0^{\Lambda_k} dk (|\Delta|^2/E)(2\pi G)$ [19], where Δ and E are gap function and quasiparticle energy in the superconductivity.

Variants of general model. Our analysis has focused on the models with rotation symmetric $j = 0$ projectors $T_{\alpha\beta\mathbf{k}}$ between different spin sectors $\alpha \neq \beta$. In fact, the model construction can be generalized to the projectors with $j > 0$. For two different spin sectors $\alpha \neq \beta$ with spins s_{α} and s_{β} , we choose the total-angular-momentum states $|v_{j_{\alpha,\beta} m_{j_{\alpha,\beta}}}^{s_{\alpha,\beta} l_{\alpha,\beta}} \mathbf{k}\rangle$ with suitable $j_{\alpha,\beta} = j$ and $l_{\alpha,\beta}$. Although these states break the rotation symmetry, the “identity” $T_{\alpha\beta\mathbf{k}} = \sum_{m_j=-j}^j k^{l_{\alpha}} |v_{jm_j\mathbf{k}}^{s_{\alpha} l_{\alpha}}\rangle \langle v_{jm_j\mathbf{k}}^{s_{\beta} l_{\beta}}| k^{l_{\beta}}$ can serve as a rotation symmetric projector for the variant models. Due to the identity structures of the projectors, the minimal band degeneracy becomes $(2j + 1)$. Particular examples include the Kane-fermion model [50–53], where two spin sectors with $(s, l, j) = (1/2, 0, 1/2)$ and $(3/2, 1, 1/2)$ are involved. The geometry of doubly degenerate bands is captured by the non-Abelian quantum metric, which does not support a quantized geometric invariant G . Another family of variant models involves the dimension reduction to 2D. This is achieved by truncating the elements with k_3 , leaving only the orbital spherical harmonics $Y_{s(\pm s)}(\hat{\mathbf{k}})$. For example, the 3D model with $(s_1, s_2) = (0, 1)$ can be reduced to the α - T_3 model in 2D [54–56]. Most of the properties can be determined

analogously to the 3D models. An important difference is the dual energy in quantum metric trace, which now takes the axial-angular-momentum form $\Lambda_{3\mathbf{k}}^2/k^2 = s_\alpha^2/k^2$ in each spin sector α [20].

Experimental realization. We briefly discuss a possible experimental realization of the $N = 2$ geometric semimetal with $(s_1, s_2) = (0, 1)$. After a unitary transformation, the Hamiltonian reads

$$\mathcal{H}_{\mathbf{k}}^{(0,1)} = \frac{1}{\sqrt{2}} \begin{pmatrix} -k_3\sqrt{2} & k_1 & k_2 & 0 \\ k_1 & 0 & 0 & k_1 \\ k_2 & 0 & 0 & k_2 \\ 0 & k_1 & k_2 & k_3\sqrt{2} \end{pmatrix}. \quad (16)$$

Interestingly, a similar four-band model [116] has recently been simulated in an experiment [46]. By employing the superconducting quantum circuits, a 4D topological semimetal was successfully investigated in a parameter space. The experimental setup involves a square lattice with four transmon qubits and four couplers, where the coupling between adjacent qubits depends on the frequency of the couplers. For the simulation of our model $\mathcal{H}_{\mathbf{k}}^{(0,1)}$, the couplers will need two suitable detuning terms and two independent sinusoidal fast-flux biases with null phases. This setup will support a straightforward mapping between the experimental parameters and the elements of $\mathcal{H}_{\mathbf{k}}^{(0,1)}$. On the other hand, an alternative setup to simulate our model lies in the ultracold atoms. By employing the atoms with suitable spin degrees of freedom, a four-band model can be simulated, as in a recent realization of the Yang monopole with rubidium-87 [49].

Conclusion and outlook. We have demonstrated the existence of geometric semimetals in 3D, which are protected by the generalized chiral and rotation symmetries. Despite trivial band topology, their nontrivial structures are uniquely characterized by the band geometry. These semimetals are thus different from the known topological ones. In future works, we will explore other possible protection symmetries, nonlinear optical responses, interaction effects, and higher-dimensional generalizations. Given the advanced techniques in the quantum-material and synthetic-matter experiments, our theoretical formalism is practically realizable with important experimental implications. Our work embraces the excitations from band geometry, thereby expanding the family of nontrivial semimetals beyond the topological realm. Furthermore, by searching for quantum phases with nontrivial geometry under trivial topology, our work paves a different way into the wide uncharted territory of unconventional quantum matter.

The authors thank Benjamin Wieder for important feedback on this Letter. Y.-P.L. acknowledges fellowship support from the Gordon and Betty Moore Foundation through the Emergent Phenomena in Quantum Systems (EPIQS) program.

* yuping.lin@berkeley.edu

† giantdomenico.palumbo@gmail.com

- [1] N. P. Armitage, E. J. Mele, and A. Vishwanath, Weyl and Dirac semimetals in three-dimensional solids, *Rev. Mod. Phys.* **90**, 015001 (2018).
- [2] X. Wan, A. M. Turner, A. Vishwanath, and S. Y. Savrasov, Topological semimetal and Fermi-arc surface states in the electronic structure of pyrochlore iridates, *Phys. Rev. B* **83**, 205101 (2011).
- [3] S. M. Young, S. Zaheer, J. C. Y. Teo, C. L. Kane, E. J. Mele, and A. M. Rappe, Dirac semimetal in three dimensions, *Phys. Rev. Lett.* **108**, 140405 (2012).
- [4] Z. Lan, N. Goldman, A. Bermudez, W. Lu, and P. Öhberg, Dirac-weyl fermions with arbitrary spin in two-dimensional optical superlattices, *Phys. Rev. B* **84**, 165115 (2011).
- [5] J. L. Mañes, Existence of bulk chiral fermions and crystal symmetry, *Phys. Rev. B* **85**, 155118 (2012).
- [6] B. J. Wieder, Y. Kim, A. M. Rappe, and C. L. Kane, Double dirac semimetals in three dimensions, *Phys. Rev. Lett.* **116**, 186402 (2016).
- [7] B. Bradlyn, J. Cano, Z. Wang, M. G. Vergniory, C. Felser, R. J. Cava, and B. A. Bernevig, Beyond dirac and weyl fermions: Unconventional quasiparticles in conventional crystals, *Science* **353**, aaf5037 (2016).
- [8] H. Isobe and L. Fu, Quantum critical points of $j = \frac{3}{2}$ dirac electrons in antiperovskite topological crystalline insulators, *Phys. Rev. B* **93**, 241113 (2016).
- [9] P. Tang, Q. Zhou, and S.-C. Zhang, Multiple types of topological fermions in transition metal silicides, *Phys. Rev. Lett.* **119**, 206402 (2017).
- [10] G. Chang, S.-Y. Xu, B. J. Wieder, D. S. Sanchez, S.-M. Huang, I. Belopolski, T.-R. Chang, S. Zhang, A. Bansil, H. Lin, and M. Z. Hasan, Unconventional chiral fermions and large topological fermi arcs in rhsi, *Phys. Rev. Lett.* **119**, 206401 (2017).
- [11] F. Flicker, F. de Juan, B. Bradlyn, T. Morimoto, M. G. Vergniory, and A. G. Grushin, Chiral optical response of multifold fermions, *Phys. Rev. B* **98**, 155145 (2018).
- [12] Z. Rao, H. Li, T. Zhang, S. Tian, C. Li, B. Fu, C. Tang, L. Wang, Z. Li, W. Fan, J. Li, Y. Huang, Z. Liu, Y. Long, C. Fang, H. Weng, Y. Shi, H. Lei, Y. Sun, T. Qian, and H. Ding, Observation of unconventional chiral fermions with long fermi arcs in cosi, *Nature* **567**, 496 (2019).
- [13] D. S. Sanchez, I. Belopolski, T. A. Cochran, X. Xu, J.-X. Yin, G. Chang, W. Xie, K. Manna, V. Süß, C.-Y. Huang, N. Alidoust, D. Multer, S. S. Zhang, N. Shumiya, X. Wang, G.-Q. Wang, T.-R. Chang, C. Felser, S.-Y. Xu, S. Jia, H. Lin, and M. Z. Hasan, Topological chiral crystals with helicoid-arc quantum states, *Nature* **567**, 500 (2019).
- [14] N. B. M. Schröter, D. Pei, M. G. Vergniory, Y. Sun, K. Manna, F. de Juan, J. A. Krieger, V. Süss, M. Schmidt, P. Dudin, B. Bradlyn, T. K. Kim, T. Schmitt, C. Cacho, C. Felser, V. N. Strocov, and Y. Chen, Chiral topological semimetal with multifold band crossings and long Fermi arcs, *Nat. Phys.* **15**, 759 (2019).
- [15] D. Takane, Z. Wang, S. Souma, K. Nakayama, T. Nakamura, H. Oinuma, Y. Nakata, H. Iwasawa, C. Cacho,

- T. Kim, K. Horiba, H. Kumigashira, T. Takahashi, Y. Ando, and T. Sato, Observation of chiral fermions with a large topological charge and associated fermi-arc surface states in *cosi*, *Phys. Rev. Lett.* **122**, 076402 (2019).
- [16] B. Q. Lv, Z.-L. Feng, J.-Z. Zhao, N. F. Q. Yuan, A. Zong, K. F. Luo, R. Yu, Y.-B. Huang, V. N. Strocov, A. Chikina, A. A. Soluyanov, N. Gedik, Y.-G. Shi, T. Qian, and H. Ding, Observation of multiple types of topological fermions in *pdBiSe*, *Phys. Rev. B* **99**, 241104 (2019).
- [17] I. Boettcher, Interplay of topology and electron-electron interactions in *rarita-schwinger-weyl* semimetals, *Phys. Rev. Lett.* **124**, 127602 (2020).
- [18] N. B. M. Schröter, S. Stolz, K. Manna, F. de Juan, M. G. Vergniory, J. A. Krieger, D. Pei, T. Schmitt, P. Dudin, T. K. Kim, C. Cacho, B. Bradlyn, H. Bormann, M. Schmidt, R. Widmer, V. N. Strocov, and C. Felser, Observation and control of maximal chern numbers in a chiral topological semimetal, *Science* **369**, 179 (2020).
- [19] Y.-P. Lin and W.-H. Hsiao, Dual haldane sphere and quantized band geometry in chiral multifold fermions, *Phys. Rev. B* **103**, L081103 (2021).
- [20] Y.-P. Lin and W.-H. Hsiao, Band geometry from position-momentum duality at topological band crossings, *Phys. Rev. B* **105**, 075127 (2022).
- [21] A. Graf and F. Piéchon, Massless multifold hopf semimetals, *Phys. Rev. B* **108**, 115105 (2023).
- [22] E.-G. Moon, C. Xu, Y. B. Kim, and L. Balents, Non-fermi-liquid and topological states with strong spin-orbit coupling, *Phys. Rev. Lett.* **111**, 206401 (2013).
- [23] T. Kondo, M. Nakayama, R. Chen, J. J. Ishikawa, E.-G. Moon, T. Yamamoto, Y. Ota, W. Malaeb, H. Kanai, Y. Nakashima, Y. Ishida, R. Yoshida, H. Yamamoto, M. Matsunami, S. Kimura, N. Inami, K. Ono, H. Kumigashira, S. Nakatsuji, L. Balents, and S. Shin, Quadratic fermi node in a 3d strongly correlated semimetal, *Nat. Commun.* **6**, 10042 (2015).
- [24] P. Zhu and R.-X. Zhang, Delicate Topology of Luttinger Semimetal, *arXiv e-prints*, [arXiv:2308.05793](https://arxiv.org/abs/2308.05793) (2023), [arXiv:2308.05793 \[cond-mat.mes-hall\]](https://arxiv.org/abs/2308.05793).
- [25] J.-M. Carter, V. V. Shankar, M. A. Zeb, and H.-Y. Kee, Semimetal and topological insulator in perovskite iridates, *Phys. Rev. B* **85**, 115105 (2012).
- [26] H. Weng, C. Fang, Z. Fang, B. A. Bernevig, and X. Dai, Weyl semimetal phase in noncentrosymmetric transition-metal monophosphides, *Phys. Rev. X* **5**, 011029 (2015).
- [27] C. Fang, Y. Chen, H.-Y. Kee, and L. Fu, Topological nodal line semimetals with and without spin-orbital coupling, *Phys. Rev. B* **92**, 081201 (2015).
- [28] Q.-F. Liang, J. Zhou, R. Yu, Z. Wang, and H. Weng, Node-surface and node-line fermions from nonsymmorphic lattice symmetries, *Phys. Rev. B* **93**, 085427 (2016).
- [29] Y. X. Zhao and Y. Lu, *PT*-symmetric real Dirac fermions and semimetals, *Phys. Rev. Lett.* **118**, 056401 (2017).
- [30] T. Bzdušek and M. Sigrist, Robust doubly charged nodal lines and nodal surfaces in centrosymmetric systems, *Phys. Rev. B* **96**, 155105 (2017).
- [31] J. Ahn, D. Kim, Y. Kim, and B.-J. Yang, Band topology and linking structure of nodal line semimetals with Z_2 monopole charges, *Phys. Rev. Lett.* **121**, 106403 (2018).
- [32] O. Türker and S. Moroz, Weyl nodal surfaces, *Phys. Rev. B* **97**, 075120 (2018).
- [33] W. Wu, Y. Liu, S. Li, C. Zhong, Z.-M. Yu, X.-L. Sheng, Y. X. Zhao, and S. A. Yang, Nodal surface semimetals: Theory and material realization, *Phys. Rev. B* **97**, 115125 (2018).
- [34] C.-K. Chiu, J. C. Y. Teo, A. P. Schnyder, and S. Ryu, Classification of topological quantum matter with symmetries, *Rev. Mod. Phys.* **88**, 035005 (2016).
- [35] K. Alpin, M. M. Hirschmann, N. Heinsdorf, A. Leonhardt, W. Y. Yau, X. Wu, and A. P. Schnyder, Fundamental laws of chiral band crossings: Local constraints, global constraints, and topological phase diagrams, *Phys. Rev. Res.* **5**, 043165 (2023).
- [36] G. Palumbo and N. Goldman, Revealing tensor monopoles through quantum-metric measurements, *Phys. Rev. Lett.* **121**, 170401 (2018).
- [37] G. Palumbo, Non-abelian tensor berry connections in multiband topological systems, *Phys. Rev. Lett.* **126**, 246801 (2021).
- [38] A. Bouhon, Q. Wu, R.-J. Slager, H. Weng, O. V. Yazyev, and T. Bzdušek, Non-abelian reciprocal braiding of weyl points and its manifestation in *zrTe*, *Nat. Phys.* **16**, 1137 (2020).
- [39] F. N. Ünal, A. Bouhon, and R.-J. Slager, Topological euler class as a dynamical observable in optical lattices, *Phys. Rev. Lett.* **125**, 053601 (2020).
- [40] A. Bouhon and R.-J. Slager, Multi-gap topological conversion of Euler class via band-node braiding: minimal models, *PT*-linked nodal rings, and chiral heirs, [arXiv:2203.16741 \[cond-mat.mes-hall\]](https://arxiv.org/abs/2203.16741).
- [41] W. J. Jankowski, M. Noormandipour, A. Bouhon, and R.-J. Slager, Disorder-induced topological quantum phase transitions in Euler semimetals, [arXiv:2306.13084 \[cond-mat.mes-hall\]](https://arxiv.org/abs/2306.13084).
- [42] A. Bouhon, Y.-Q. Zhu, R.-J. Slager, and G. Palumbo, Second Euler number in four dimensional synthetic matter, [arXiv:2301.08827 \[cond-mat.mes-hall\]](https://arxiv.org/abs/2301.08827).
- [43] Z. Wang, B. J. Wieder, J. Li, B. Yan, and B. A. Bernevig, Higher-order topology, monopole nodal lines, and the origin of large Fermi arcs in transition metal dichalcogenides *XTe₂* ($X = \text{Mo}, \text{W}$), *Phys. Rev. Lett.* **123**, 186401 (2019).
- [44] G. Salerno, N. Goldman, and G. Palumbo, Floquet-engineering of nodal rings and nodal spheres and their characterization using the quantum metric, *Phys. Rev. Res.* **2**, 013224 (2020).
- [45] X. Tan, D.-W. Zhang, Z. Yang, J. Chu, Y.-Q. Zhu, D. Li, X. Yang, S. Song, Z. Han, Z. Li, Y. Dong, H.-F. Yu, H. Yan, S.-L. Zhu, and Y. Yu, Experimental measurement of the quantum metric tensor and related topological phase transition with a superconducting qubit, *Phys. Rev. Lett.* **122**, 210401 (2019).
- [46] Y. Zhang, Y.-Q. Zhu, J. Xu, W. Zheng, D. Lan, G. Palumbo, N. Goldman, S.-L. Zhu, X. Tan, Z. Wang, and Y. Yu, Exploring parity magnetic effects through quantum simulation with superconducting qubits, *Phys. Rev. Appl.* **21**, 034052 (2024).
- [47] M. Yu, P. Yang, M. Gong, Q. Cao, Q. Lu, H. Liu, S. Zhang, M. B. Plenio, F. Jelezko, T. Ozawa, N. Goldman, and J. Cai, Experimental measurement of the quantum geometric tensor using coupled qubits in di-

- amond, *Nat. Sci. Rev.* **7**, 254 (2019).
- [48] M. Chen, C. Li, G. Palumbo, Y.-Q. Zhu, N. Goldman, and P. Cappellaro, A synthetic monopole source of kalbramond field in diamond, *Science* **375**, 1017 (2022).
- [49] S. Sugawa, F. Salces-Carcoba, A. R. Perry, Y. Yue, and I. B. Spielman, Second chern number of a quantum-simulated non-abelian yang monopole, *Science* **360**, 1429 (2018).
- [50] M. Orlita, D. M. Basko, M. S. Zholudev, F. Teppe, W. Knap, V. I. Gavrilenko, N. N. Mikhailov, S. A. Dvoretckii, P. Neugebauer, C. Faugeras, A.-L. Barra, G. Martinez, and M. Potemski, Observation of three-dimensional massless kane fermions in a zinc-blende crystal, *Nat. Phys.* **10**, 233 (2014).
- [51] J. D. Malcolm and E. J. Nicol, Magneto-optics of massless kane fermions: Role of the flat band and unusual berry phase, *Phys. Rev. B* **92**, 035118 (2015).
- [52] K. Gadge, S. Tewari, and G. Sharma, Anomalous hall and nernst effects in kane fermions, *Phys. Rev. B* **105**, 235420 (2022).
- [53] S. S. Krishtopenko and F. Teppe, Relativistic collapse of landau levels of kane fermions in crossed electric and magnetic fields, *Phys. Rev. B* **105**, 125203 (2022).
- [54] D. Bercioux, N. Goldman, and D. F. Urban, Topology-induced phase transitions in quantum spin hall lattices, *Phys. Rev. A* **83**, 023609 (2011).
- [55] A. Raoux, M. Morigi, J.-N. Fuchs, F. Piéchon, and G. Montambaux, From dia- to paramagnetic orbital susceptibility of massless fermions, *Phys. Rev. Lett.* **112**, 026402 (2014).
- [56] T. Louvet, P. Delplace, A. A. Fedorenko, and D. Carpentier, On the origin of minimal conductivity at a band crossing, *Phys. Rev. B* **92**, 155116 (2015).
- [57] J. P. Provost and G. Vallee, Riemannian structure on manifolds of quantum states, *Commun. Math. Phys.* **76**, 289 (1980).
- [58] D. N. Page, Geometrical description of berry's phase, *Phys. Rev. A* **36**, 3479 (1987).
- [59] J. Anandan and Y. Aharonov, Geometry of quantum evolution, *Phys. Rev. Lett.* **65**, 1697 (1990).
- [60] Y.-Q. Ma, S. Chen, H. Fan, and W.-M. Liu, Abelian and non-abelian quantum geometric tensor, *Phys. Rev. B* **81**, 245129 (2010).
- [61] N. Marzari and D. Vanderbilt, Maximally localized generalized wannier functions for composite energy bands, *Phys. Rev. B* **56**, 12847 (1997).
- [62] T. Neupert, C. Chamon, and C. Mudry, Measuring the quantum geometry of bloch bands with current noise, *Phys. Rev. B* **87**, 245103 (2013).
- [63] M. Kolodrubetz, V. Gritsev, and A. Polkovnikov, Classifying and measuring geometry of a quantum ground state manifold, *Phys. Rev. B* **88**, 064304 (2013).
- [64] R. Roy, Band geometry of fractional topological insulators, *Phys. Rev. B* **90**, 165139 (2014).
- [65] S. Peotta and P. Törmä, Superfluidity in topologically nontrivial flat bands, *Nat. Commun.* **6**, 8944 (2015).
- [66] Y. Gao, S. A. Yang, and Q. Niu, Geometrical effects in orbital magnetic susceptibility, *Phys. Rev. B* **91**, 214405 (2015).
- [67] F. Piéchon, A. Raoux, J.-N. Fuchs, and G. Montambaux, Geometric orbital susceptibility: Quantum metric without berry curvature, *Phys. Rev. B* **94**, 134423 (2016).
- [68] C. H. Lee, M. Claassen, and R. Thomale, Band structure engineering of ideal fractional chern insulators, *Phys. Rev. B* **96**, 165150 (2017).
- [69] G. Palumbo, Momentum-space cigar geometry in topological phases, *Eur. Phys. J. Plus* **133**, 23 (2018).
- [70] O. Bleu, G. Malpuech, Y. Gao, and D. D. Solnyshkov, Effective theory of nonadiabatic quantum evolution based on the quantum geometric tensor, *Phys. Rev. Lett.* **121**, 020401 (2018).
- [71] L. Asteria, D. T. Tran, T. Ozawa, M. Tarnowski, B. S. Rem, N. Fläschner, K. Sengstock, N. Goldman, and C. Weitenberg, Measuring quantized circular dichroism in ultracold topological matter, *Nat. Phys.* **15**, 449 (2019).
- [72] A. Marrazzo and R. Resta, Local theory of the insulating state, *Phys. Rev. Lett.* **122**, 166602 (2019).
- [73] Y.-Q. Zhu, W. Zheng, S.-L. Zhu, and G. Palumbo, Band topology of pseudo-hermitian phases through tensor berry connections and quantum metric, *Phys. Rev. B* **104**, 205103 (2021).
- [74] H. Weisbrich, G. Rastelli, and W. Belzig, Geometrical rabi oscillations and landau-zener transitions in non-abelian systems, *Phys. Rev. Res.* **3**, 033122 (2021).
- [75] O. Pozo and F. de Juan, Computing observables without eigenstates: Applications to bloch hamiltonians, *Phys. Rev. B* **102**, 115138 (2020).
- [76] K.-E. Huhtinen, J. Herzog-Arbeitman, A. Chew, B. A. Bernevig, and P. Törmä, Revisiting flat band superconductivity: Dependence on minimal quantum metric and band touchings, *Phys. Rev. B* **106**, 014518 (2022).
- [77] J. Herzog-Arbeitman, V. Peri, F. Schindler, S. D. Huber, and B. A. Bernevig, Superfluid weight bounds from symmetry and quantum geometry in flat bands, *Phys. Rev. Lett.* **128**, 087002 (2022).
- [78] C. Northe, G. Palumbo, J. Sturm, C. Tutschku, and E. M. Hankiewicz, Interplay of band geometry and topology in ideal chern insulators in the presence of external electromagnetic fields, *Phys. Rev. B* **105**, 155410 (2022).
- [79] A. Graf and F. Piéchon, Berry curvature and quantum metric in n -band systems: An eigenprojector approach, *Phys. Rev. B* **104**, 085114 (2021).
- [80] T. Ozawa and N. Goldman, Extracting the quantum metric tensor through periodic driving, *Phys. Rev. B* **97**, 201117 (2018).
- [81] T. Ozawa and B. Mera, Relations between topology and the quantum metric for chern insulators, *Phys. Rev. B* **104**, 045103 (2021).
- [82] B. Mera and T. Ozawa, Kähler geometry and chern insulators: Relations between topology and the quantum metric, *Phys. Rev. B* **104**, 045104 (2021).
- [83] B. Mera and J. Mitscherling, Nontrivial quantum geometry of degenerate flat bands, *Phys. Rev. B* **106**, 165133 (2022).
- [84] J. Wang, J. Cano, A. J. Millis, Z. Liu, and B. Yang, Exact landau level description of geometry and interaction in a flatband, *Phys. Rev. Lett.* **127**, 246403 (2021).
- [85] J. Wang, S. Klevtsov, and Z. Liu, Origin of model fractional chern insulators in all topological ideal flatbands: Explicit color-entangled wave function and exact density algebra, *Phys. Rev. Res.* **5**, 023167 (2023).
- [86] V. Kozii, A. Avdoshkin, S. Zhong, and J. E. Moore, Intrinsic anomalous hall conductivity in a nonuniform electric field, *Phys. Rev. Lett.* **126**, 156602 (2021).
- [87] A. Avdoshkin and F. K. Popov, Extrinsic geometry of

- quantum states, *Phys. Rev. B* **107**, 245136 (2023).
- [88] J. Ahn, G.-Y. Guo, and N. Nagaosa, Low-frequency divergence and quantum geometry of the bulk photovoltaic effect in topological semimetals, *Phys. Rev. X* **10**, 041041 (2020).
- [89] J. Ahn, G.-Y. Guo, N. Nagaosa, and A. Vishwanath, Riemannian geometry of resonant optical responses, *Nat. Phys.* **18**, 290 (2022).
- [90] H.-C. Hsu, J.-S. You, J. Ahn, and G.-Y. Guo, Nonlinear photoconductivities and quantum geometry of chiral multifold fermions, *Phys. Rev. B* **107**, 155434 (2023).
- [91] G. von Gersdorff and W. Chen, Measurement of topological order based on metric-curvature correspondence, *Phys. Rev. B* **104**, 195133 (2021).
- [92] A. Abouelkomsan, K. Yang, and E. J. Bergholtz, Quantum metric induced phases in moiré materials, *Phys. Rev. Res.* **5**, L012015 (2023).
- [93] M. S. M. de Sousa, A. L. Cruz, and W. Chen, Mapping quantum geometry and quantum phase transitions to real space by a fidelity marker, *Phys. Rev. B* **107**, 205133 (2023).
- [94] T. Holder, D. Kaplan, and B. Yan, Consequences of time-reversal-symmetry breaking in the light-matter interaction: Berry curvature, quantum metric, and diabatic motion, *Phys. Rev. Res.* **2**, 033100 (2020).
- [95] X. Hu, T. Hyart, D. I. Pikulin, and E. Rossi, Quantum-metric-enabled exciton condensate in double twisted bilayer graphene, *Phys. Rev. B* **105**, L140506 (2022).
- [96] S. Panahiyan, W. Chen, and S. Fritzsche, Fidelity susceptibility near topological phase transitions in quantum walks, *Phys. Rev. B* **102**, 134111 (2020).
- [97] A. Gianfrate, O. Bleu, L. Dominici, V. Ardizzone, M. De Giorgi, D. Ballarini, G. Lerario, K. W. West, L. N. Pfeiffer, D. D. Solnyshkov, D. Sanvitto, and G. Malpuech, Measurement of the quantum geometric tensor and of the anomalous hall drift, *Nature* **578**, 381 (2020).
- [98] M. Thumin and G. Bouzerar, Flat-band superconductivity in a system with a tunable quantum metric: The stub lattice, *Phys. Rev. B* **107**, 214508 (2023).
- [99] T. B. Smith, L. Pullasserri, and A. Srivastava, Momentum-space gravity from the quantum geometry and entropy of Bloch electrons, *Phys. Rev. Res.* **4**, 013217 (2022).
- [100] P. J. Ledwith, A. Vishwanath, and D. E. Parker, Vortexability: A unifying criterion for ideal fractional Chern insulators, *Phys. Rev. B* **108**, 205144 (2023).
- [101] B. Hetényi and P. Lévy, Fluctuations, uncertainty relations, and the geometry of quantum state manifolds, *Phys. Rev. A* **108**, 032218 (2023).
- [102] X. Ni, M. Weiner, A. Alù, and A. B. Khanikaev, Observation of higher-order topological acoustic states protected by generalized chiral symmetry, *Nat. Mater.* **18**, 113 (2019).
- [103] S. N. Kempkes, M. R. Slot, J. J. van den Broeke, P. Capiod, W. A. Benalcazar, D. Vanmaekelbergh, D. Bercioux, I. Swart, and C. Morais Smith, Robust zero-energy modes in an electronic higher-order topological insulator, *Nat. Mater.* **18**, 1292 (2019).
- [104] T. Morimoto and A. Furusaki, Weyl and Dirac semimetals with \mathbb{Z}_2 topological charge, *Phys. Rev. B* **89**, 235127 (2014).
- [105] B.-J. Yang, T. Morimoto, and A. Furusaki, Topological charges of three-dimensional Dirac semimetals with rotation symmetry, *Phys. Rev. B* **92**, 165120 (2015).
- [106] S.-J. Huang, J. Yu, and R.-X. Zhang, Classification of Interacting Dirac Semimetals, *arXiv e-prints*, arXiv:2211.03802 (2022), arXiv:2211.03802 [cond-mat.str-el].
- [107] C. Guo, L. Hu, C. Putzke, J. Diaz, X. Huang, K. Manna, F.-R. Fan, C. Shekhar, Y. Sun, C. Felser, C. Liu, B. A. Bernevig, and P. J. W. Moll, Quasi-symmetry-protected topology in a semi-metal, *Nature Physics* **18**, 813 (2022).
- [108] L.-H. Hu, C. Guo, Y. Sun, C. Felser, L. Elcoro, P. J. W. Moll, C.-X. Liu, and B. A. Bernevig, Hierarchy of quasisymmetries and degeneracies in the *cosi* family of chiral crystal materials, *Phys. Rev. B* **107**, 125145 (2023).
- [109] T. T. Wu and C. N. Yang, Dirac monopole without strings: Monopole harmonics, *Nucl. Phys. B* **107**, 365 (1976).
- [110] T. T. Wu and C. N. Yang, Some properties of monopole harmonics, *Phys. Rev. D* **16**, 1018 (1977).
- [111] R. Shankar, Quantum geometry and topology, in *Topology and Condensed Matter Physics*, edited by S. M. Bhattarjee, M. Mj, and A. Bandyopadhyay (Springer Singapore, Singapore, 2017) pp. 253–279.
- [112] F. D. M. Haldane, Fractional quantization of the Hall effect: A hierarchy of incompressible quantum fluid states, *Phys. Rev. Lett.* **51**, 605 (1983).
- [113] J. K. Jain, *Composite Fermions* (Cambridge University Press, Cambridge, 2007).
- [114] W.-H. Hsiao, Landau quantization of multilayer graphene on a Haldane sphere, *Phys. Rev. B* **101**, 155310 (2020).
- [115] See Supplemental Material at [URL] for the linear injection conductivity in geometric semimetals.
- [116] Y.-Q. Zhu, N. Goldman, and G. Palumbo, Four-dimensional semimetals with tensor monopoles: From surface states to topological responses, *Phys. Rev. B* **102**, 081109 (2020).

Supplemental Material for “Geometric semimetals and their simulation in synthetic matter”

I. LINEAR INJECTION CONDUCTIVITY IN GEOMETRIC SEMIMETALS

Here, for simplicity, we consider our simplest four-band model, namely $\mathcal{H}_{\mathbf{k}}^{(0,1)}$ with a tilting term. Its momentum-space Hamiltonian is given by

$$\mathcal{H}_{\mathbf{k}}^{(0,1)}(v_t, \mu) = k_i T^i + (\mu + v_t k_x) \mathcal{I}, \quad (\text{S1})$$

where \mathcal{I} is the 4×4 identity matrix, $k_i = \{k_x, k_y, k_z\}$, μ is the chemical potential, v_t is related to the tilt of the Dirac-like cone along the x -direction and

$$T^x = \begin{pmatrix} 0 & \frac{1}{\sqrt{2}} & 0 & 0 \\ \frac{1}{\sqrt{2}} & 0 & 0 & \frac{1}{\sqrt{2}} \\ 0 & 0 & 0 & 0 \\ 0 & \frac{1}{\sqrt{2}} & 0 & 0 \end{pmatrix}, \quad T^y = \begin{pmatrix} 0 & 0 & \frac{1}{\sqrt{2}} & 0 \\ 0 & 0 & 0 & 0 \\ \frac{1}{\sqrt{2}} & 0 & 0 & \frac{1}{\sqrt{2}} \\ 0 & 0 & \frac{1}{\sqrt{2}} & 0 \end{pmatrix}, \quad T^z = \begin{pmatrix} -1 & 0 & 0 & 0 \\ 0 & 0 & 0 & 0 \\ 0 & 0 & 0 & 0 \\ 0 & 0 & 0 & 1 \end{pmatrix}. \quad (\text{S2})$$

Its spectrum is given by

$$E_1 = (\mu + v_t k_x) - \sqrt{k_x^2 + k_y^2 + k_z^2}, \quad E_2 = (\mu + v_t k_x), \\ E_3 = (\mu + v_t k_x), \quad E_4 = (\mu + v_t k_x) + \sqrt{k_x^2 + k_y^2 + k_z^2}. \quad (\text{S3})$$

The corresponding eigenvectors are real and for this reason all the Berry connections are null. However, the Abelian quantum metric is not null. In particular for the eigenvector V_1 of the lower band $n = 1$ we have

$$g_{ij} = \partial_i V_1^T \partial_j V_1, \quad (\text{S4})$$

and its components are explicitly given by

$$g_{xy} = -\frac{k_x k_y}{2(k_x^2 + k_y^2 + k_z^2)^2}, \quad g_{xx} = \frac{k_y^2 + k_z^2}{2(k_x^2 + k_y^2 + k_z^2)^2}, \quad g_{yy} = \frac{k_x^2 + k_z^2}{2(k_x^2 + k_y^2 + k_z^2)^2}, \\ g_{zz} = \frac{k_x^2 + k_y^2}{2(k_x^2 + k_y^2 + k_z^2)^2}, \quad g_{xz} = -\frac{k_x k_z}{2(k_x^2 + k_y^2 + k_z^2)^2}, \quad g_{yz} = -\frac{k_y k_z}{2(k_x^2 + k_y^2 + k_z^2)^2}, \quad (\text{S5})$$

which do not depend neither of the tilting parameter v_t nor of the chemical potential μ . We have that

$$g_{jj} = g_{xx} + g_{yy} + g_{zz} = \frac{1}{|k|^2}, \quad (\text{S6})$$

which is in agreement with our general result in the main text. In terms of physical observables, we now compute the linear injection in our system. In fact, the quantum metric appears also in several non-linear optical responses. In particular, the linear effect is compatible with space-time inversion PT symmetry, while other non-linear effects such as the circular injection are zero due to the absence of a non-zero Berry curvature. Following Ref. [88], we want now to study the linear injection in our model. The linear injection is a nonlinear response compatible with PT symmetry and is related by the change of the electron velocity during the inter-band transition of electrons induced by an oscillating external electric field. It is given by

$$\sigma^{c,ab} = -\tau \frac{2\pi e^3}{\hbar^2} \int \frac{d^3 k}{(2\pi)^3} \sum_{n,m} f_{nm} \Delta_{mn}^c r_{nm}^b r_{mn}^a \delta(E_{mn} - \omega), \quad (\text{S7})$$

where τ represents the relaxation time that saturates the injection current, δ is the Dirac delta function, ω is the frequency associated to the external electric field, $f_{nm} = f_n - f_m$, where f_n is the Fermi-Dirac distribution of the band n , $E_{mn} = E_m - E_n$ is the energy difference, $\Delta_{mn}^c = v_{mm}^c - v_{nn}^c$ is the inter-band transition of the velocity with

n the occupied bands and m the non-occupied ones. Moreover, $r_{mn}^a = V_m^T i \partial_a V_n$ are the cross gap Berry connections, with V_n the corresponding eigenvectors for the band n . The above expression can be equivalently written in spherical coordinates (θ, ϕ) as follows

$$\sigma^{c,ab} = -\tau \frac{2\pi e^3}{\hbar^2} \int_{E_{cv}=\omega} \frac{d\theta d\phi \sin \phi |k|^2}{(2\pi)^3} (\hat{n} \cdot \hat{c}) g_{ab}^n, \quad (\text{S8})$$

because $\Delta_{mn}^c = \partial_c E_{mn}$ such that $\Delta_{mn}^c \delta(E_{mn} - \omega) = \partial_c \Theta(E_{mn} - \omega)$, with Θ the step function and e the electric charge. Here, g_{ab}^n is the quantum metric of the occupied band $n = 1$ and the \hat{n} is the normal vector of the surface. Because the trace of the quantum metric is $1/|k|^2$ as showed previously, the linear injection trace reads

$$\sigma^{c,aa} = -\tau \frac{e^3}{\hbar^2} \int_{E_{cv}=\omega} d\theta d\phi \sin \phi (\hat{n} \cdot \hat{c}), \quad (\text{S9})$$

where the integral depends only of the shape of the Fermi surface, which is completely determined by v_t , μ and ω . We notice that for the un-tilted case (i.e. $v_t = 0$), the surface is a sphere and the above integral is then zero having $\hat{n} = (\sin \phi \cos \theta, \sin \phi \sin \theta, \cos \phi)$. Thus, tilted cones in geometric semimetals are characterized by a non-zero Fermi-surface-dependent linear injection trace. This is in contract with spin-s Weyl semimetals with tilted Weyl cones, which are also characterized by a circular injection due to the presence of a non-zero Berry curvature. Thus, there exist suitable non-linear physical observables that can naturally distinguish three-dimensional geometric semimetals from three-dimensional topological semimetals.